ACS APPLIED BIO MATERIALS

Article

www.acsabm.org

IL-10 Gene Transfection in Primary Endothelial Cells via Linear and Branched Poly(β-amino ester) Nanoparticles Attenuates Inflammation in Stimulated Macrophages

Nicholas DiStasio,[†,‡] Marloes Arts,[†,‡] Stephanie Lehoux,[*,‡] and Maryam Tabrizian[*,†]

[†]Department of Biomedical Engineering, McGill University, 3773 University, Montréal, QC H3A 2B6, Canada

[‡]Lady Davis Institute, Department of Medicine, McGill University, 3755 Chemin de la Côte-Sainte-Catherine, Montréal, QC H3T 1E2, Canada

Supporting Information

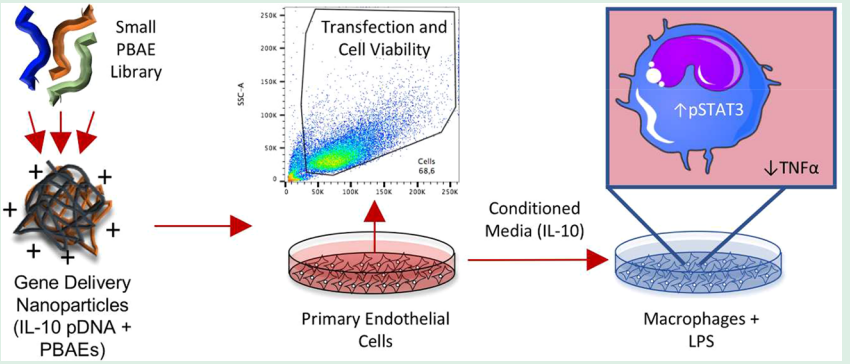

ABSTRACT: Poly(β-amino esters) or PBAEs are highly efficient synthetic polymers optimized for gene delivery, a complicated process dependent on polymer properties such as hydrophobicity, charge, and degradability. The modular design of PBAEs has allowed for the identification of which polymer and nanoparticle properties significantly affect gene delivery efficiency in various cell types. However, these investigations need to be extended to more difficult-to-transfect cells such as primary endothelial cells, which hold enormous potential for atherosclerosis. Here a small library of 6 different PBAEs were screened for efficacy and safety in two types of primary endothelial cells (ECs). Nearly all polymers were more efficient than commercial transfection reagents ($p < 0.05$), reaching 60% and 15% transfection efficiency in human and mouse primary ECs, respectively. The top performing PBAE was used to deliver a plasmid encoding the anti-inflammatory cytokine interleukin-10 (IL-10), which has the potential to reduce inflammation in atherosclerosis. Significant increases in IL-10 mRNA and protein were detectable in ECs 72 h after transfection with PBAE:IL-10 nanoparticles. Macrophages cultured in conditioned medium from IL10-transfected ECs showed activation of anti-inflammatory signaling pathways. In addition, these macrophages secreted significantly less (25%) tumor necrosis factor α (TNFα) when challenged with lipopolysaccharide (LPS). These results underline the capabilities of PBAEs to be expanded as a fine-tunable platform for anti-inflammatory gene delivery within the context of atherosclerosis.

KEYWORDS: *atherosclerosis, polymer nanoparticles, gene therapy, interleukin-10, endothelial cells, macrophages*

1.0. INTRODUCTION

Poly(β-amino esters) or PBAEs are biodegradable synthetic polymers used for gene delivery due to their excellent transfection abilities that have been illustrated in various cell types.[1] These cationic PBAEs condense anionic plasmid DNA into polymer:DNA nanoparticles (NPs) or polyplexes via electrostatic interactions and have been synthesized in thousands of permutations. Electrostatic interactions are strong enough to hold complexes together in physiological conditions, but ester bonds within PBAEs degrade rapidly to release DNA once inside the cell. Thus, the top-performing PBAEs exhibit a delicate balance between hydrophobicity and cationic charge,[2] which are mainly influenced by the choice of end-capping amine group.[3,4] PBAEs with branched structures have also been reported to increase gene transfection, likely due to the increased density of end-capping groups.[5,6] However, the majority of studies utilizing PBAEs have been performed in relatively easy-to-transfect cell types, such as Chinese hamster ovary (CHO), COS-7, and human embryonic kidney (HEK293).

Relatively few studies have shown successful transfection using linear PBAEs in the more difficult-to-transfect endothelial cells (ECs),[7−9] with no studies yet reported on branched PBAEs in endothelial cells. The difficulty in

Received: July 19, 2018
Accepted: August 16, 2018
Published: August 16, 2018

DOI: 10.1021/acsabm.8b00342
ACS Appl. Bio Mater. XXXX, XXX, XXX−XXX

transfecting ECs arises mainly because of their confluent resting state and low rate of division, which restricts access to the nucleus.[10] In addition, ECs secrete a negatively charged, highly sulfated matrix-like film known as the glycocalyx that further inhibits nanoparticle uptake.[11] Despite these difficulties, they remain a desirable target for gene delivery in cardiovascular disease (CVD), the leading cause of mortality in western society.[12] Indeed, ECs have been targeted in previous studies for imaging and the delivery of therapeutics for atherosclerosis, the leading cause of clinical events in CVD.[13−15] As ECs overlie the atherosclerotic plaque, they secrete chemokines, cytokines, microRNAs, and growth factors that influence monocyte recruitment and differentiation into macrophages, which cultivate the chronic inflammation that drives atherosclerosis.[16]

Atherosclerosis is characterized by the accumulation of lipid-laden cells in a pro-inflammatory milieu where cytokines and matrix-degrading enzymes create a complex plaque that is prone to rupture. The formation and progression of atherosclerotic plaques are driven in part by the nuclear factor-κB (NF-κB) signaling pathway, which is activated in endothelial cells and macrophages among other cell types.[17,18] Many of the downstream products of NF-κB signaling, such as the prototypical pro-inflammatory cytokine TNFα, can be offset by anti-inflammatory cytokines such as IL-10.[19] In mouse models, the overexpression or delivery of IL-10 has been shown to attenuate the inflammation involved in atherosclerosis,[20−23] though nonviral delivery of IL-10 in atherosclerosis has not yet been reported. IL-10 intervenes with many processes that drive plaque progression, such as the inhibition of NF-κB signaling[24] and the increase in efflux of lipids from macrophages that prevents the formation of foam cells.[25] IL-10 mainly acts by binding the IL-10 receptors (IL-10R1 and IL-10R2), which induces their dimerization and activates the receptor-associated kinases, janus kinase 1 (JAK1) and tyrosine kinase 2 (Tyk2).[26,27] These activated kinases phosphorylate signal transducer and activator of transcription 3 (STAT3), which leads to the transcription of downstream genes that have been implicated in attenuating inflammation in the M1 macrophage phenotype.[28,29]

Thus, the objective of this study was to identify a PBAE capable of efficient transfection of IL-10 in primary endothelial cells by screening six linear and branched PBAEs. The top-performing PBAE NP was then applied in a proof-of-concept anti-inflammatory study within the context of atherosclerosis. The results of this study suggest that NP-mediated delivery of an anti-inflammatory gene to ECs can attenuate inflammation in macrophages whose accumulation and pro-inflammatory phenotype drive atherosclerotic plaque progression.

2.0. MATERIALS AND METHODS

2.1. Materials. The following materials were purchased and used as received: 1,4-butanediol diacrylate ("C"), 5-amino-1-pentanol ("32"), trimethylol propane triacrylate ("TMPTA"), 1,3-diaminopropane (DAP), 1,3-diaminopentane (PDA), anhydrous DMSO and diethyl ether from Sigma-Aldrich, Canada, 1-(3-aminopropyl)-4-methylpiperazine (PiP) and polyethylenimine (linear, 25 kDa and branched, 10 kDa) from Alfa Aesar (Haverhill, MA, USA), and Lipofectamine 3000 from Thermo-Fisher Scientific Canada.

2.1.1. Plasmids. Detailed descriptions for the synthesis and characterization plasmids used can be found in the Supporting Information (SI).

2.2. Polymer Synthesis and Characterization. Linear PBAEs were synthesized as reported previously[9,30] by mixing monomers "C" and "32" at an acrylate-to-amine molar ratio of 1.2:1. Briefly, 345 mg (3.3 mmol) of "C" was mixed with 800 mg (4 mmol) of prewarmed (liquid) "32" without solvent in a 1-dram glass vial and stirred in an oven at 90 °C for 24 h to form the linear C32 base polymer. The C32 base polymer was end-capped with DAP or PDA by mixing 321 mg of 31.13% (w/w) C32 in DMSO with 800 μL of a 0.25 M solution of DAP or PDA in DMSO. For end-capping with PiP, 480 μL of a 167 mg/mL solution of C32 in DMSO was added to 320 μL of 0.5 M PiP in DMSO. All end-capping reactions were incubated overnight on a shaker at room temperature and protected from light.

Branched PBAEs were formed by mixing 500 mg/mL solutions of "C", prewarmed liquid "32", and TMPTA in anhydrous DMSO as described previously.[31] Amounts of 1.32 g of (6.66 mmol) "C", 0.66 g (6.4 mmol) of "32", and 0.19 g (0.66 mmol) of TMPTA were mixed together to maintain an acrylate-to-amine ratio of 1.2:1 with 10% branching.[6] Monomers were stirred for 48 h in an oven at 90 °C and then end-capped as mentioned above for the linear PBAEs. Linear and branched PBAEs were precipitated in 3 volumes of ether, vortexed, and centrifuged at 2000*g* for 5 min before decanting the ether. Ether purification was repeated 2×, and polymers were dried under vacuum for 24−48 h. Dry polymers were dissolved in anhydrous DMSO (100 mg/mL) and aliquoted into light-impermeable tubes and stored at −20 °C with desiccant. The polymer structures were confirmed with ^{1}H NMR on a 400 MHz AVIIIHD 400 spectrometer (Bruker, Billerica, MA, USA) in chloroform-*d* (Cambridge Isotope Laboratories Inc., Tewskbury, MA, USA), and the spectra were analyzed with TopSpin (Bruker). M_w was determined by gel permeation chromatography, which was performed on a Waters Breeze GPC system (Milford, MA, USA) with 717 autosampler, 2414 refractive index (RI) detector, and 1525 binary HPLC pump in anhydrous tetrahydrofuran (Sigma-Aldrich, Canada). M_w was determined against polystyrene standards.

2.3. Nanoparticle Formation and Characterization. Nanoparticles were formed by diluting both pDNA and PBAEs in 25 mM sodium acetate buffer (pH = 5.2 ± 0.2). PBAEs were diluted to 1.8 or 3.6 mg/mL from 100 mg/mL stock solutions, while pDNA was diluted to 60 μg/mL. To obtain nanoparticles with PBAE:pDNA ratios of 30 or 60 w/w, one volume of each PBAE solution was added to 1 volume of pDNA solution and vortexed 10 s followed by a 10 min incubation before characterization or cell transfection. DLS measurements were performed on a Brookhaven ZetaPals analyzer (Holtsville, NY, USA). The nanoparticles were diluted 1/5 in PBS for size measurements and 1/5 in 25 mM acetate buffer for zeta potential measurements.

2.4. Cell Culture. Pooled donor human umbilical vein endothelial cells (HUVECs, Lonza #C2519A) were cultured in growth medium (1:1 mixture of EGM-2 (Lonza, Canada #CC-3162) and DMEM-F12 (Wisent, QC, Canada) containing 10% FBS, 1% penicillin/streptomycin (P/S)). HUVECs were grown in culture plates coated with 0.1% gelatin (EMD Millipore #ES-006-B) and used before passage 5 for all experiments. Murine endothelial cells (mECs) were isolated from the lungs of C57BL/6 mice between 7 and 10 weeks of age as described previously.[32] Briefly, mice were sacrificed by CO_2 asphyxiation, and lungs were macerated using surgical scissors under sterile conditions and incubated 1 h at 37 °C in serum-free RPMI 1640 (Wisent) supplemented with 1% P/S and 0.1% Collagenase A (Roche Diagnostics, Laval, QC, Canada). The media containing tissue chunks was passed through a 16G needle 15×, and then a 100 μm cell strainer, and was centrifuged at 226*g* for 5 min. The cell pellet was resuspended in growth media in a 75 cm^2 flask precoated with 0.1% gelatin. The growth medium was refreshed every 2−4 days until cells reached confluency (7−10 days). mECs were then immuno-isolated with sheep antirat IgG Dynabeads (Invitrogen, #11035) that were conjugated to a rat antimouse CD102 antibody (BD Biosciences #553325). Before isolation, 10 μL magnetic beads were washed 3× in 2% BSA-PBS and incubated with 10 μL (10 μg) of CD102 antibody for 3 h at 4 °C. The washing step was repeated 3×, and the beads were added to mECs in T75 flasks followed by a 1 h incubation at 4 °C. Cells were then washed, trypsinized, and passed over a magnet (EMD Millipore, Canada, PureProteome #LSKMAGS15). Unbound

DOI: 10.1021/acsabm.8b00342
ACS Appl. Bio Mater. XXXX, XXX, XXX−XXX

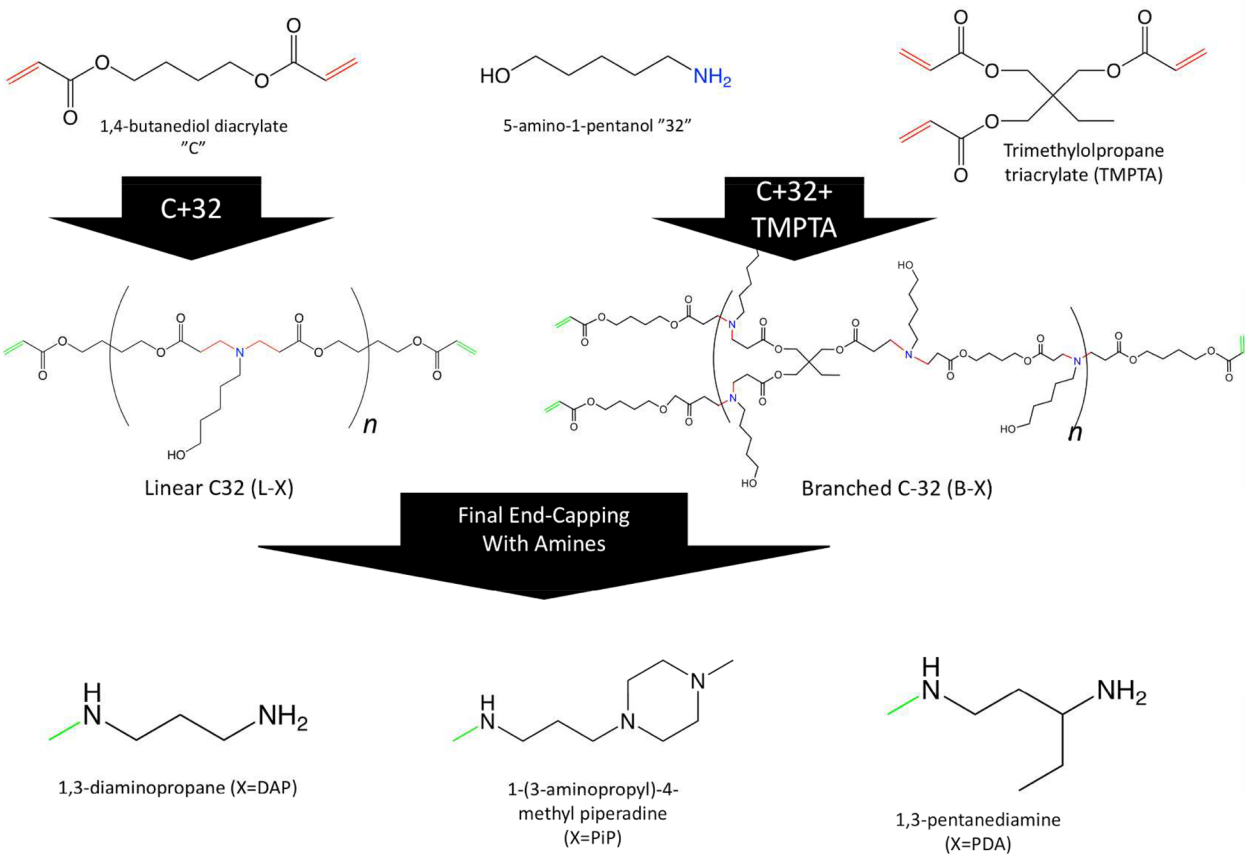

Figure 1. Synthesis pathways used to create acrylate-terminated linear (L) and branched (B) C32 base polymers, which were then reacted with each small molecule amine (DAP, PiP, or PDA) to end-cap free acrylate groups.

cells and media were carefully removed, and magnetically fixed cells were resuspended in growth media and plated onto gelatin-coated flasks. After letting the isolated ECs grow until confluency (7−12 days), a second immunoisolation was performed as above to yield a pure population of mECs, which were used between passages 3 and 6. RAW264.7 macrophages were a gift from Talin Ebrahimian and were cultured in RPMI 1640 (Wisent) supplemented with 10% FBS and 1% P/S.

2.5. Flow Cytometry. For flow cytometry experiments, HUVECs and mECs were plated in 12-well plates precoated with a 0.1% gelatin solution with 80 000 cells/well for HUVECs and 65 000 cells/well for mECs 24 h before transfection. Nanoparticles formed between PBAEs and pMAX-GFP were made as described in section 2.2 and added directly to the wells (total of 3 μg pGFP/well). The medium was refreshed after 4 h. Identical treatments with Lipofectamine 3000 and polyethylenimine (PEI) (3:1 w/w ratio to pDNA) per manufacturer recommendations were used as positive controls, and pDNA alone in acetate buffer was added as a negative control.

After 48 h, cells were washed 2× with PBS, trypsinized, suspended in FACS buffer (PBS + 2% BSA), and centrifuged at 250g, for 5 min, at 4 °C. The cells were washed once more with PBS before being resuspended in FACS buffer. DAPI (1.67 μg/mL final conc.) was added 5−10 min before tubes were analyzed in the flow cytometer to exclude dead cells. Flow experiments were performed on the LSRFortessa (BD Biosciences, San Jose, CA, USA) flow cytometer with 488 nm laser (530/30 filter) for GFP fluorescence and 405 nm laser (450/50 filter) for DAPI. Data were then analyzed using FlowJo (BD Biosciences). Singlets were gated in both forward and side scatter to avoid analyzing aggregates.

2.6. Isolation of IL-10 Conditioned Media (CM). mECs were seeded into gelatin-coated 6-well plates (0.2 × 10^6 cells/well) 24 h before nanoparticle transfection was performed using the same protocol as mentioned above, but the pMAX-GFP plasmid was replaced with either the pIRES2-EGFP-IL10 or pIRES2-EGFP (negative control plasmid without IL-10 coding insert) at 5 μg of pDNA/well. 72 h after transfection, supernatant was collected and centrifuged at 23 700g and 4 °C for 15 min. It was then filtered (0.2 μm) and stored at −20 °C.

2.7. Quantitative Reverse Transcription PCR (qPCR). mRNA was isolated from mECs 72 h after transfection. The cells were washed once with cold PBS on ice and then scraped into cold RBC lysis buffer (included in Geneaid kit, 100 μL). RNA was then purified using the Total RNA Mini Kit (Geneaid) mentioned in the Supporting Information (SI), transcribed into cDNA as mentioned in the Supporting Information (SI), and qPCR was carried out using SYBR green (Applied Biosystems, Foster City, CA, USA) as per manufacturer protocols to quantify RNA copies on an ABI 7500 fast real-time PCR system (Applied Biosystems). Gene expression was compared to housekeeping ribosomal protein 16 (Rps16). The following primers were used: *IL-10* forward 5′- GTGATGCCC-CAAGCTGAGA-3′ and reverse 5′-CACGGCCTTGCTCTTGTTTT-3′; *Rps16* forward 5′- ATCT-CAAAGGCCCTGGTAGC-3′ and reverse 5′- ACAAAGG-TAAACCCCGATCC-3′.

2.8. Attenuation of Inflammation in RAW264.7 Macrophages. RAW264.7 macrophages were seeded in a 48-well plate at 62.5 × 10^3 cells/well in RPMI 1640. After sufficient time for the cells to attach, at least 4 h, they were serum starved in low serum RPMI 1640 (0.5% FBS, 1% P/S) overnight. RPMI was removed, and conditioned media containing IL-10 or not depending on mEC transfection conditions was then added (1 mL/well) in addition to LPS when indicated (10 or 100 ng/mL). The cells were returned to the incubator for 24 h. Media was then collected and stored at −20 °C for ELISA assays of TNFα production.

2.9. Activation of Anti-Inflammatory Signaling in RAW264.7 Macrophages. RAW 264.7 macrophages were seeded into 6-well

DOI: 10.1021/acsabm.8b00342
ACS Appl. Bio Mater. XXXX, XXX, XXX−XXX

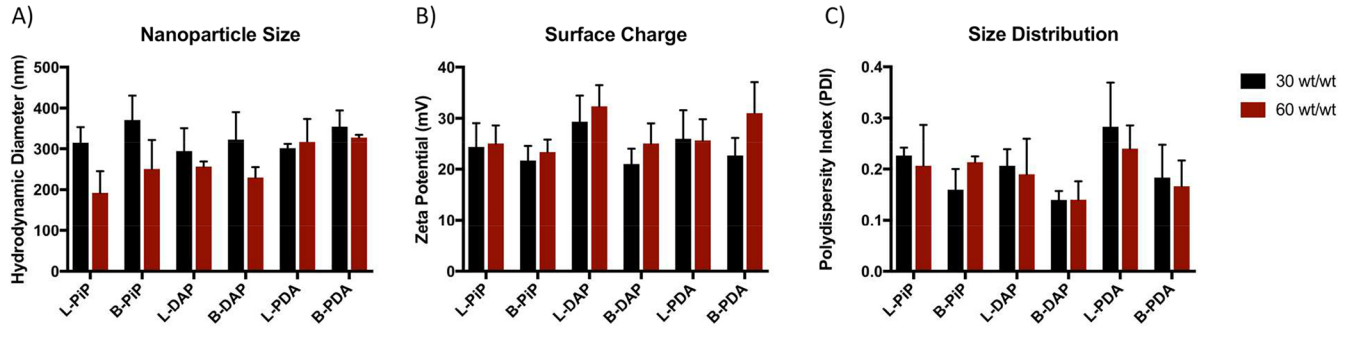

D)

Parameter Measured	Size	Charge	PDI
Branching	n.s.	n.s.	*p=0.0104
Polymer End Group	*p=0.0463	n.s.	n.s.
Wt/Wt ratio	*p=0.0171	n.s.	n.s.

Figure 2. Nanoparticle physicochemical characterization via dynamic light spectroscopy displaying the (A) size, (B) surface charge, and (C) polydispersity of PBAE:pEGFP nanoparticles. (D) Table describing significant effects of fine-tunable properties (polymer branching, end group, or weight ratio of polymer:DNA). Statistical testing was performed using either paired *t* tests (branching and wt ratio) or matched one-way ANOVA (polymer end group). $N = 3$ for all, ns = not significant, $*p < 0.05$.

plates (0.5×10^6 cells/well) in RPMI (10% FBS, 1% penicillin/streptomycin) and then serum starved overnight in low serum RPMI (0.5% FBS, 1% penicillin/streptomycin). An amount of 1 mL of CM (±IL-10 depending on EC transfection conditions) was added to macrophages along with proteasome inhibitor MG-132 (Sigma-Aldrich) to further inhibit protein degradation. Cells were incubated for 4 h and then placed on ice, washed 3× with cold PBS, and scraped into 80 μL of cell lysis buffer, which contained the following ingredients in 10 mL: final concentrations of 50 mM Na pyrophosphate, 50 mM NaF, 5 mM NaCl, 5 mM Na2 EDTA, 5 mM EGTA, 10 mM HEPES, and 0.5% Triton X-100; 1 tablet antiproteases cOmplete mini (Roche Diagnostics); and Na_3VO_4 (2 mM final concentration). Cells were lysed using a probe tip sonicator (Sonics Vibra-cell, Newtown, CT, USA) for 3 s (1 s on, 1 s off) and then centrifuged 23 700*g*, at 4 °C, for 15 min. Supernatants were placed in a fresh tube and stored until use at −80 °C. An amount of 30 μg of total protein (as quantified by BCA assay) was added per well in a 10% SDS-PAGE gel and transferred to nitrocellulose membranes. The following antibodies were used as per manufacturer instructions: rabbit antiphospho-STAT3 (Y705, Cell Signaling Technologies #9145, 1/2000), mouse anti-STAT3 (Transduction Laboratories #610190, 1/1000), antimouse or antirabbit HRP (1/2000, BioRad #172-1011 and 170-6515, respectively). Visualization was performed using Western Lightning ECL Pro (PerkinElmer) chemiluminescent substrate, and membranes were imaged on a ChemiDoc XRS+ (BioRad, Hercules, CA, USA). Band intensities were quantified using ImageJ.

2.10. Enzyme-Linked Immunosorbent Assay (ELISA). ELISA kits were obtained from Thermo Fisher Scientific, and assays were performed as per manufacturer instructions on cell supernatants undiluted or diluted 1:10 in EliSPOT diluent (included in kit) to be in sensitivity ranges: 10−150 pg/mL for IL-10 (#88-7106-22) and 10−300 pg/mL for mouse TNFα (#88-7324-22).

2.11. Statistics. Statistical analysis was performed in Graphpad Prism 7 software (Graphpad Software, La Jolla, CA, USA). Paired student's *t* tests and/or matched one-way ANOVA were used to test the effects of branching, polymer wt/wt ratio to pDNA, and end group chosen on physicochemical properties, cell transfection, and viability. One-way ANOVA with Sidak's multiple comparisons test was used to test transfection conditions for all PBAEs against lipofectamine as well as for cell viability against pDNA only control. Unpaired student's *t* test was used to compare effects of CM ± IL-10 for qPCR, ELISA, and Western blot results. All data are presented as mean ± SEM with $p < 0.05$ denoted "*" and $p < 0.01$ denoted "#".

3.0. RESULTS

3.1. Synthesis and Characterization of Linear and Branched PBAEs. PBAEs are formed via the Michael's addition polymerization reaction "neat" without the use of catalysts or other reagents. The syntheses were confirmed via ^{1}H NMR spectroscopy. Base polymer end-capping was verified by the disappearance of acrylate peaks around 5.0−5.8 ppm (Figure S1).[33] The M_w was then quantified by gel permeation chromatography (GPC). The M_w's of linear and branched PBAEs were 5.3 kDa (polydispersity index (PDI) of 1.49) and 6.2 kDa (PDI of 1.91), respectively (Table S1).

3.2. Synthesis and Characterization of PBAE:pDNA NPs. NPs were formed with the 6 PBAEs at two different weight ratios of polymer to pDNA to compare the effect of 3 different parameters on NP physicochemical properties and transfection efficiency in primary endothelial cells. These parameters were (1) the effect of branching the polymer structure, (2) the weight ratio of polymer to pDNA, and (3) the choice of end-capping amine group (Figure 1).

Nanoparticles are formed via the electrostatic interactions between cationic PBAEs and anionic plasmid DNA. Because of the excess of cationic PBAEs to pDNA in complexation, nanoparticles are cationic. Two weight ratios of polymer:-pDNA were chosen based on preliminary experiments. It was discovered that of 10, 30, 60, and 100 w/w ratios of PBAEs to pDNA, 30 and 60 w/w bound all pDNA available and prevented its migration in an agarose gel electrophoresis test for all PBAEs (data not shown), whereas 10 and 100 w/w were unable to complex fully with pDNA. Nanoparticles formed between all PBAEs and pMAX-GFP were used for physicochemical characterization measurements, although those formed with the pIRES2-EGFP-IL10 plasmid had similar properties for the same PBAE (data not shown).

Figure 2 shows the physicochemical properties of NPs including which formulation (i.e., fine-tunable) parameters have a significant impact on physicochemical properties. The

DOI: 10.1021/acsabm.8b00342
ACS Appl. Bio Mater. XXXX, XXX, XXX−XXX

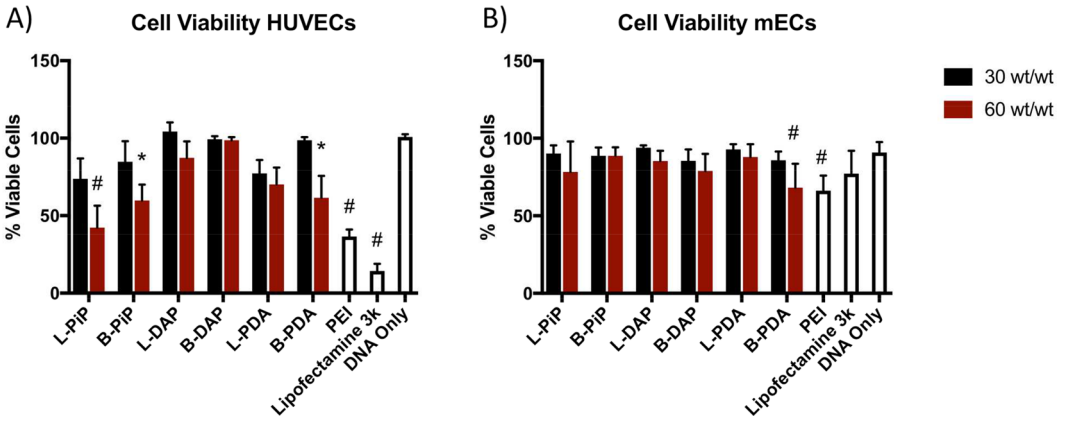

Figure 3. Cell viability of PBAE:pEGFP nanoparticles in two primary endothelial cell lines: (A) HUVECs and (B) mouse mECs as measured by DAPI exclusion via flow cytometry. $N \geq 3$ for HUVECs, and N = mECs from at least 4 mice. *$p < 0.05$ and #$p < 0.01$ when compared to DNA only control.

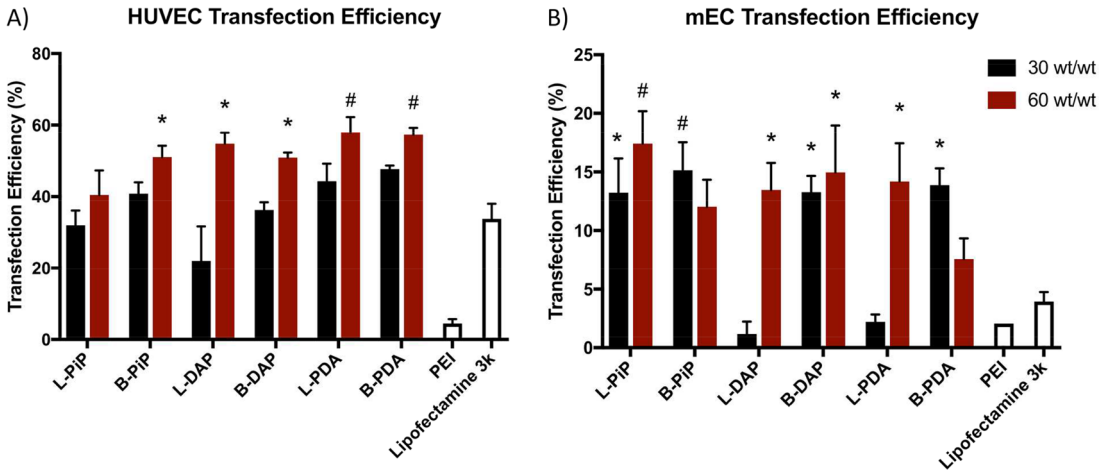

Figure 4. Transfection efficiency of PBAE:pEGFP nanoparticles in two primary endothelial cell lines: (A) HUVECs and (B) mECs as measured by percentage of GFP+ cells over other living (DAPI−) cells via flow cytometry. $N \geq 3$ for HUVECs, and N = mECs from at least 4 mice. *$p < 0.05$ and #$p < 0.01$ when compared to Lipofectamine 3k via one-way ANOVA with Sidak's multiple comparison's test.

size of NPs was the most variable parameter (Figure 2A), being influenced by both the end group chosen and the w/w ratio of PBAE:pDNA. Interestingly, with the three controllable NP formation parameters tested, none led to a significant change in the surface charge of particles (Figure 2B). Similarly, the polydispersity index (PDI) was only significantly affected by branching the structure of PBAEs wherein branched PBAEs formed more monodisperse nanoparticles (Figure 2C). These results are summarized in Figure 2D.

3.3. Effects of Polymer Structure and Amount on NP Toxicity and Transfection Efficiency in Primary Endothelial Cells. To acquire a more complete understanding of how PBAEs behave in primary ECs, two types of ECs were chosen. HUVECs have been used before in transfection studies and served to relate the findings of this study with those in the literature. Mouse pulmonary ECs (mECs) were chosen to determine the limits of PBAE transfection capabilities in a new and challenging primary mouse EC model.

First, the viability of ECs was assayed after exposure to PBAE:pGFP NPs for all polymers and controls. The majority of PBAE:pEGFP nanoparticles did not cause significant cell death in either HUVECs (Figure 3A) or mECs (Figure 3B). In HUVECs, L-PiP-60, B-PiP-60, and B-PDA-60 displayed significant toxicity over control. mECs seemed to be more robust as only B-PDA-60 resulted in toxicity. Both cell types experienced significant toxicity from standard transfection reagent PEI, whereas commercial reagent Lipofectamine was significantly toxic in HUVECs only. These results underline the importance of screening materials in specific cell types as they may react differently.

To characterize the transfection efficiency of the polymers, NPs at both 30 and 60 w/w ratios were freshly prepared using the pMAX-GFP plasmid and added to both HUVECs and mECs. In Figure 4A, the transfection efficiency in HUVECs was markedly higher (~60% for best performing PBAEs) than in mECs (~15%, Figure 4B). L-PiP-60 was most efficient for mECs, whereas the 60 wt ratio PDA-terminated PBAEs were most efficient for HUVECs (L-PDA-60 and B-PDA-60). Branching the structure of PBAEs had little effect on their transfection efficiency. Some slight improvements were seen with branching for HUVECs (-PiP and -DAP polymers) but not in mECs. However, at a 30 w/w ratio, L-DAP and L-PDA were not efficient in transfecting mECs, but the branched versions showed significant improvement (Figure 4B). Five of the PBAEs showed transfection efficiency significantly higher than the positive control Lipofectamine 3k for HUVECs.

All transfection methods (Lipofectamine and PBAEs) were less efficient in mECs than HUVECs; however, nearly all (8/

DOI: 10.1021/acsabm.8b00342
ACS Appl. Bio Mater. XXXX, XXX, XXX−XXX

12) PBAEs showed significantly greater efficiency than Lipofectamine (Figure 4B). Polyethylenimine (PEI, linear 25 kDa) was also included as it is a synthetic polymer often used in gene transfection studies, but it was not very efficient for primary endothelial cells.

Table 1 summarizes the effect of NP structure and amount (wt ratio) on cell viability and transfection efficiency in the two types of primary endothelial cells investigated. Integrating the results for transfection efficiency, cell viability, and nanoparticle properties, the L-PiP-30 polymer was selected for anti-inflammatory gene therapy studies involving IL-10 in mECs. There was a general increase in transfection with 60 wt ratios for PBAEs in HUVECs accompanied by an increase in cell death, but this was not observed in mECs (Table 1).

Table 1. Contributions of Fine-Tunable Parameters of NP Formation on Cell Viability and Transfection Efficiency for HUVECs and mECs[a]

parameter	cell viability (mEC)	transfection efficiency (mEC)	cell viability (HUVEC)	transfection efficiency (HUVEC)
branching	0.2319	0.4767	0.1688	0.1138
polymer end group	0.6933	0.2900	*0.0118	0.0971
wt/wt ratio	*0.021	0.3203	*0.0188	*0.0101

[a]Data are p-values showing significant differences between groups (parameters) as measured by paired student's t-test (branching and wt/wt ratio) and by matched one-way ANOVA (polymer end group), $N \geq 3$ for HUVECs and N = mECs from at least 4 mice $^*p < 0.05$.

3.4. mEC Transfection and Production of IL-10 Using L-PiP-30 Nanoparticles. Detailed synthesis and description of the pIRES2-EGFP-IL10 plasmid are given in the Supporting Information (SI). This plasmid was used as a means to produce the anti-inflammatory protein IL-10 in primary endothelial cells. The production of IL-10 was visualized in HUVECs via GFP from the same RNA transcript as IL-10 in this plasmid (Figure S2). Since HUVECs had higher transfection efficiencies, they also produced higher amounts of IL-10 than mECs (~35 ng/mL vs ~0.8 ng/mL in mECs) (Figure S3). However, mECs were the focus of anti-inflammatory studies as they are a new *ex vivo* cell type. To first characterize the production of IL-10 by transfected mECs, quantitative real-time PCR (qPCR) was performed after 72 h of transfection with L-PiP-30. Figure 5 shows a significant increase in IL-10 production when mECs are transfected using L-PiP-30 PBAE nanoparticles containing the pIRES2-EGFP-IL10 plasmid (NPs + IL-10) vs the same plasmid without the IL-10 insert (NPs-IL-10). A significant increase in IL-10 mRNA production was observed (Figure 5A) when normalizing to the expression of housekeeping Rps16 protein. This translated to a significant increase in IL-10 protein production (851 ± 39 pg/mL) in the conditioned media from transfected mECs after 72 h (Figure 5B) as measured by ELISA.

3.5. Conditioned Media (CM) from IL10-Transfected Primary Endothelial Cells Activates Anti-Inflammatory Pathways in RAW264.7 Macrophages. IL-10 was successfully produced via L-PiP-30 NP transfections at both the mRNA and protein level in mECs. Thus, the anti-inflammatory activity of CM containing IL-10 was evaluated in mouse macrophages via functional assays. First, a prototypical signaling pathway of IL-10 was examined, namely, the phosphorylation of STAT3.[34] CM from mECs transfected with pIRES2-EGFP plasmid (CM -IL10) or pIRES2-EGFP-IL10 plasmid (CM + IL10) was added to RAW264.7 macrophages. After 4 h in CM + IL10, there was a 2-fold increase in the phosphorylation of STAT3, normalized to the expression of total unphosphorylated STAT3 (Figure 6). Thus, media derived from IL10-transfected mECs activated a canonical IL-10 anti-inflammatory signaling pathway in macrophages.

3.6. CM from IL10-Transfected Primary Endothelial Cells Reduces Inflammation in Stimulated RAW264.7 Macrophages. After verifying that CM from IL10-transfected mECs activates anti-inflammatory pathways in macrophages, it was then determined if a functional macrophage response to pro-inflammatory stimuli could be observed. Within the atherosclerotic plaque, activated (pro-inflammatory) macrophages secrete damaging cytokines, such as TNFα, that perpetuate inflammation and destabilize the plaque. For macrophage activation, lipopolysaccharide (LPS) derived from bacterial cell walls was chosen. LPS induces a well-characterized hyperactive inflammatory response via toll-like receptors 2 and 4 (TLR-2/-4) in RAW264.7 macrophages.[35] When macrophages were cultured in CM -IL10 without LPS stimulation, there was a very low baseline of TNFα production as measured by ELISA (41 ± 14 pg/mL) (Figure 7). TNFα levels increased to 1167 ± 351 pg/mL when 10 ng/mL of LPS (+) was added and substantially increased to 2060 ± 195 pg/mL when 100 ng/mL of LPS was added (++), indicating a dose-dependent response (Figure 7, black bars). CM + IL10

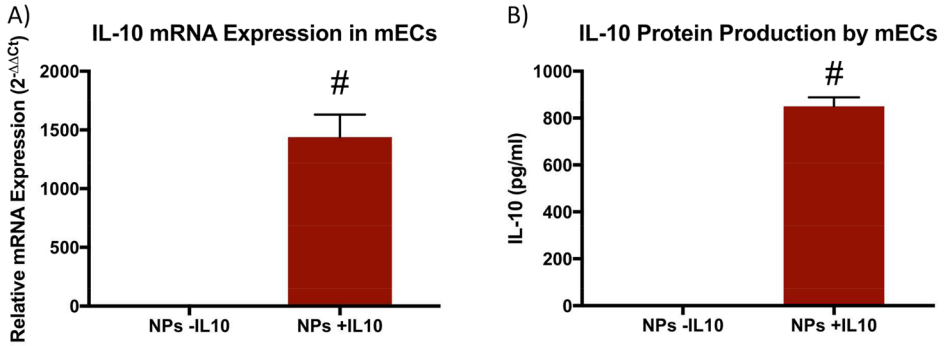

Figure 5. Quantitation of IL-10 production in mECs following transfection with L-PiP-30 and pIRES2-EGFP-IL10 or pIRES2-EGFP plasmids. (A) mRNA production was normalized to housekeeping gene Rps16 via qPCR. (B) IL-10 protein levels were detected in supernatant via ELISA. All analysis was done 72 h after transfection (N = mECs from at least 4 mice, #$p < 0.01$, via student's t test).

DOI: 10.1021/acsabm.8b00342
ACS Appl. Bio Mater. XXXX, XXX, XXX−XXX

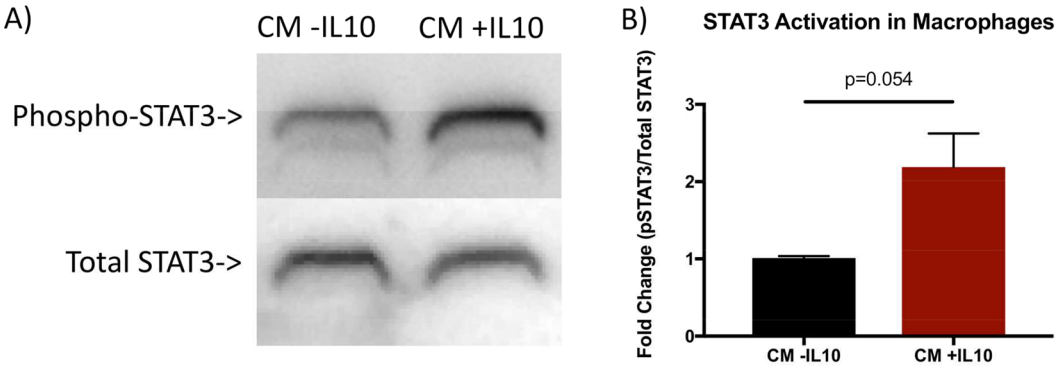

Figure 6. Conditioned media from IL10-transfected mECs increases phospho-STAT3 in macrophages. (A) Expression of phosphorylated STAT3 normalized to total nonphosphorylated STAT3. Image representative of three independent experiments, quantified in (B). Statistics evaluated by student's *t*-test with *N* = CM from 3 sets of mECs on 3 independent batches of RAW264.7 macrophages.

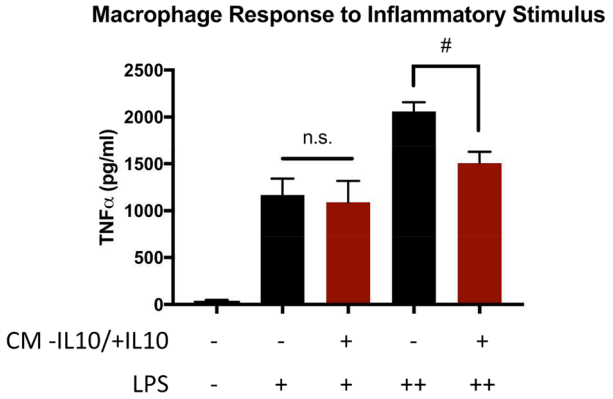

Figure 7. TNFα secretion by RAW264.7 macrophages in CM in response to LPS stimulation for 24 h. 10 ng/mL LPS (+); 100 ng/mL LPS (++). Data are mean ± SEM, #$p < 0.01$ from one-way ANOVA with Dunnett's Multiple Comparisons test, *N* = CM from 4 sets of mECs. TNFα levels measured via ELISA.

had no impact on TNFα production in response to 10 ng/mL of LPS. However, CM + IL10 significantly attenuated TNFα production in macrophages stimulated with 100 ng/mL of LPS ($p < 0.01$), compared to CM-IL10. Hence, CM + IL10 displayed a high potential to attenuate the production of pro-inflammatory cytokines in stimulated macrophages.

4.0. DISCUSSION

Biodegradable polymers, and PBAEs specifically, offer unique advantages by virtue of their combinatorial and solvent-free synthesis which can allow for transfection and toxicity investigations in a variety of cell types. Along these lines, a small library of 6 PBAEs were synthesized by adding 3 different end-capping groups (PiP, DAP, and PDA) onto the linear C32 base polymer (L) or the branched C32-TMPTA base polymer (B). The molecular weight of the linear PBAEs was similar to previous reports in the literature, while the branched PBAEs in this study were slightly smaller (6.2 kDa vs 10+ kDa reported to be successful by others[36−40]). However, studies have shown that linear PBAE performance is most affected by the end group chosen in easier-to-transfect cells,[30] whereas molecular weight may play a larger role in branched PBAEs.[41] High performing end groups for branched PBAEs have included 1,11-diamino-3,6,9-trioxaundecane[6] and 3-morpholinopropylamine.[37,38,41]

The end groups in this study were selected for their ability to provide consistently high transfection efficiencies in various cell types[30,42,43] including endothelial cells. Similarly, the branched version of C32 was included in the library to test whether branching could improve endothelial cell transfection as branched PBAEs have been shown to increase transfection efficiency over their linear counterparts in other cell types.[6] Thus, the polymer library in this study consisted of 3 top-performing linear PBAEs (L-PiP, L-DAP, L-PDA) identified from the literature (involving ECs where available[7,9,43]) and the branched counterparts, some of which were synthesized for the first time here (B-PiP and B-PDA). The effect of polymer amount was also considered by testing each PBAE at two different weight ratios to DNA since transfection generally increases with increasing polymer amount; however, toxicity generally increases as well.[44] In terms of the physicochemical properties of NPs, it was discovered that both the polymer:-pDNA wt ratio and end group chosen could significantly influence NP size, whereas no parameter influenced the surface charge of NPs, in agreement with others.[30] Nanoparticles are considered very small (10−100 nm range); however, polyplexes are often larger (150+ nm) and have still seen success *in vivo*.[45] Larger particles may extravasate more efficiently to the endothelium in blood flow which holds promise for new strategies to target atherosclerosis using polyplexes.[46,47] In terms of polyplex dispersity, a significant decrease was observed when moving from linear to branched PBAEs, indicating that branching could help achieve more monodisperse NPs. This has not been reported in studies involving branched PBAEs as PDI does not seem to be a parameter explored in previous studies.

Few PBAEs significantly increased primary EC death in this study, and only at the higher wt/wt ratio of 60:1 polymer to DNA. While the linear PBAEs are often used at 30:1 and 60:1, previous studies involving branched PBAEs[37,38] typically used lower ratios (10:1, 20:1, and 30:1). However, wt/wt ratios of 30 and 60:1 were chosen for branched PBAEs in this study for direct comparison with linear counterparts. It is possible that branched PBAEs could be more effective in mECs at lower doses (10:1 or 20:1), and this was one limitation to the study. Despite the many weight ratios that have been tested *in vitro*, the corresponding *in vivo* doses of NPs rarely exceed 30 w/w for the typical 25−50 μg plasmid DNA in the literature.[48−50]

Interestingly, branching the structure of PBAEs led to few differences in physicochemical characteristics or transfection efficiency/toxicity of these nanoparticles in primary ECs. It is

DOI: 10.1021/acsabm.8b00342
ACS Appl. Bio Mater. XXXX, XXX, XXX−XXX

possible that these cells present higher transection barriers even for the branched polymers, which were shown to be superior to linear PBAEs in easier-to-transfect cells such as HEK293, CHO, and COS-7 cells.[31] Indeed, the best performing polymers in this study reached a maximum of 60% transfection efficiency in HUVECs, a result shared by others.[9,51] In addition, the HUVECs seemed to respond more to branched PBAEs (Table 1), and the most efficient polymer for HUVECs was not the best for mECs. As mECs are taken directly from mice in an in-house protocol and HUVECs are from a commercial provider, differences in their responses to potential treatments can be expected. Nevertheless, branching the base polymer structure was able to facilitate transfection in some conditions where linear PBAEs were unsuccessful in mECs (L-DAP-30 and L-PDA-30). Taken together, these data indicate a high dependence of cell type on transfection efficiency and the degree to which it can be enhanced.

As mentioned earlier, there were few statistical differences between the branched and linear PBAEs in terms of NP properties, cell viability, and cell transfection, although the B-PiP polymer performed slightly better than the L-PiP in mEC transfection (17 ± 3% vs 13 ± 3%). However, this was not a significant difference, and the choice for L-PiP was made more based on minor advantages of L-PiP over B-PiP. For example, L-PiP generally formed smaller nanoplexes with pDNA (~300 nm for L-PiP vs ~380 nm for B-PiP), which could be desirable for future *in vivo* studies. In addition, as L- and B-PiP performed nearly identically, L-PiP only uses two monomers and no organic solvents for its synthesis, which can save money and waste. Therefore, L-PiP was chosen as the lead polymer for subsequent anti-inflammatory experiments involving IL-10 gene delivery.

IL-10 has been widely recognized as a potent anti-inflammatory protein with high therapeutic potential. Known originally as cytokine synthesis inhibitory factor, its involvement in the resolution of inflammation is ubiquitous in infection,[52] fibrosis,[53] atherosclerosis,[54] and many other pathologies mainly through acting on macrophages. To deliver IL-10, the pIRES2-EGFP plasmid was chosen, which allows for translation of the gene of interest along with a GFP reporter. Though GFP expression in the pIRES2-EGFP plasmid is not as high as in typical reporter plasmids,[55] the GFP expression can be used to monitor successful transfections under the microscope in live cells. The production of IL-10 was also confirmed at both the mRNA and protein level.

The main pathway activated and responsible for the anti-inflammatory effects of IL-10 is STAT3, which acts to both produce anti-inflammatory proteins[28,56] and as a negative feedback element, shutting down the inflammatory response.[29] CM from IL10-transfected cells induced a robust response in RAW264.7 macrophages in the form of STAT3 phosphorylation. Some pSTAT3 was observed in response to CM from GFP control cells as well, indicating that the mEC secretome may also activate STAT3, though not as potently as in IL10-transfected cells. However, the EC media itself (which contains many growth factors) did not activate STAT3, showing the specificity of EC-derived factors (data not shown).

Though significant, the effects of IL-10 within conditioned media in this study were not as large as those reported in the many studies using RAW264.7 macrophages and recombinant IL-10 protein. Clarke et al. observed that 1 ng/mL or higher of IL-10 reduced the production of TNFα in macrophages incubated with 10 ng/mL LPS.[57] In contrast, IL-10 measured in mEC CM in this study reached only ~0.8 ng/mL, and a significant anti-inflammatory response was only observed upon LPS stimulation at 100 ng/mL. Interestingly, no effect on TNFα secretion was observed after macrophages were incubated in CM + IL10 and a lower dose of LPS (10 ng/mL). This may suggest that some threshold value of inflammation must be achieved before evidence of IL-10 activity can be seen or that IL-10 can only lower TNFα secretion to a certain level. Inflammatory signaling thresholds have been discussed in the literature previously.[58] It is unlikely that the timing of IL-10 exposure is a determining factor in the poor response to LPS at 10 ng/mL since, both in this study (data not shown) and others,[19] administering IL-10 (recombinant or in CM from mECs) 15 min to 2 h prior to LPS produced the same subsequent reduction in TNFα.

In terms of mechanism of action, IL-10 CM-mediated attenuation of TNFα production in response to LPS implicated no change in TNFα mRNA levels (data not shown), indicating a possible post-translational effect. Clarke et al.[57] reported similar findings. In fact, the mRNA levels of MMP-9 and ICAM-1 were also examined in this study and found to be elevated by LPS but similarly unchanged in CM + IL10 (data not shown). This contrasts with data from Hovsepian et al.,[52] who observed an IL-10-dependent decrease in mRNA levels of TNFα, as well as IL-6, MMP-9, and MMP-2 after infection with *T. Cruzi* in cardiomyocytes. Perhaps differences are due to the inflammatory stimulation method (whole bacteria vs LPS) or cell type (cardiac muscle cells vs ECs). These results further outline the complexity and exciting capabilities of the immune response.

5.0. CONCLUSIONS

This study compared the effects of branching, end-group modification, and weight ratio of polymer to pDNA on NP formation and physicochemical properties. The small library of 6 different PBAE NPs were also evaluated for DNA transfection efficiency and viability in two types of primary endothelial cells (mECs and HUVECs) as models for difficult-to-transfect cell types. In mECs, none of the varied parameters significantly affected transfection efficiency, while in HUVECs, the ratio of polymer to DNA in the NPs had a significant effect on transfection efficiency with higher ratios resulting in better transfection, but also more toxicity. The viability of both HUVECs and mECs generally decreased with increasing polymer to DNA ratios, while the polymer's end-capping group affected only the HUVECs' viability. Therefore, the HUVECs were more responsive to changes in polymer properties than the mECs. The top-performing PBAE for HUVECs (B-PiP-60) was different than that for mECs (L-PiP-30). Hence, screening a small library of PBAEs such as this was useful as even these two types of primary endothelial cells showed marked differences in gene expression and toxicity.

The best-performing PBAE in mECs was used to deliver the IL-10 gene, which resulted in production of IL-10 at both the mRNA and protein level. When CM from IL-10 transfected mECs was applied to murine macrophages, a 2-fold increase in the phosphorylation of STAT3 was observed. Furthermore, the IL-10 containing CM caused a 25% reduction in the secretion of TNFα by LPS-stimulated macrophages. This study was a promising first step toward finding an optimal material for the nonviral transfection of primary ECs and the modification of their immediate environment via protein secretion. ECs are involved in various diseases, and their immediate environment

DOI: 10.1021/acsabm.8b00342
ACS Appl. Bio Mater. XXXX, XXX, XXX−XXX

often contains important effector cells like macrophages, such as in the case of atherosclerosis. Though nonviral DNA delivery has been utilized in atherosclerosis to lower lipid levels,[59] no such anti-inflammatory gene delivery strategies have been attempted.

■ ASSOCIATED CONTENT

Supporting Information

The Supporting Information is available free of charge on the ACS Publications website at DOI: 10.1021/acsabm.8b00342.

Experimental procedures for the synthesis of all plasmids used, polymer characterization data (^{1}H NMR spectrographs), molecular weight data table (GPC), HUVEC expression of pIRES2-EGFP-IL10 via fluorescence microscopy, and IL-10 production via PBAE transfection of HUVECs (PDF)

■ AUTHOR INFORMATION

Corresponding Authors

*E-mail: maryam.tabrizian@mcgill.ca.

*E-mail: stephanie.lehoux@mcgill.ca.

ORCID

Nicholas DiStasio: 0000-0001-8846-6523

Maryam Tabrizian: 0000-0002-5050-4480

Notes

The authors declare no competing financial interest.

■ ACKNOWLEDGMENTS

The authors graciously thank David Simon and Talin Ebrahimian for help in planning experiments, Sylvain Essiembre for GPC measurements, and Emily Buck for help with manuscript editing. S.L. is financed by an operating grant from the Canadian Institutes of Health Research, and M.T. is funded by grants from both the Canadian Institutes for Health Research and the National Sciences and Engineering Research Council of Canada.

■ REFERENCES

(1) Green, J. J.; Langer, R.; Anderson, D. G. A Combinatorial Polymer Library Approach Yields Insight Into Nonviral Gene Delivery. *Acc. Chem. Res.* **2008**, *41*, 749−759.

(2) Bishop, C. J.; Kozielski, K. L.; Green, J. J. Exploring the Role of Polymer Structure on Intracellular Nucleic Acid Delivery Via Polymeric Nanoparticles. *J. Controlled Release* **2015**, *219*, 488−499.

(3) Sunshine, J. C.; Akanda, M. I.; Li, D.; Kozielski, K. L.; Green, J. J. Effects of Base Polymer Hydrophobicity and End-Group Modification on Polymeric Gene Delivery. *Biomacromolecules* **2011**, *12*, 3592−3600.

(4) Keeney, M.; Ong, S.-G.; Padilla, A.; Yao, Z.; Goodman, S.; Wu, J. C.; Yang, F. Development of Poly(B-Amino Ester)-Based Biodegradable Nanoparticles for Nonviral Delivery of Minicircle DNA. *ACS Nano* **2013**, *7*, 7241−7250.

(5) Cheng, W.; Wu, D.; Liu, Y. Michael Addition Polymerization of Trifunctional Amine and Acrylic Monomer: A Versatile Platform for Development of Biomaterials. *Biomacromolecules* **2016**, *17*, 3115−3126.

(6) Zhou, D.; Gao, Y.; O'Keeffe Ahern, J.; A, S.; Xu, Q.; Huang, X.; Greiser, U.; Wang, W. Development of Branched Poly(5-Amino-1-Pentanol-Co-1,4-Butanediol Diacrylate) With High Gene Transfection Potency Across Diverse Cell Types. *ACS Appl. Mater. Interfaces* **2016**, *8*, 34218−34226.

(7) Shmueli, R. B.; Sunshine, J. C.; Xu, Z.; Duh, E. J.; Green, J. J. Gene Delivery Nanoparticles Specific for Human Microvasculature and Macrovasculature. *Nanomedicine* **2012**, *8*, 1200−1207.

(8) Cho, S.-W.; Yang, F.; Son, S. M.; Park, H.-J.; Green, J. J.; Bogatyrev, S.; Mei, Y.; Park, S.; Langer, R.; Anderson, D. G. Therapeutic Angiogenesis Using Genetically Engineered Human Endothelial Cells. *J. Controlled Release* **2012**, *160*, 515−524.

(9) Green, J. J.; Zugates, G. T.; Tedford, N. C.; Huang, Y. H.; Griffith, L. G.; Lauffenburger, D. A.; Sawicki, J. A.; Langer, R.; Anderson, D. G. Combinatorial Modification of Degradable Polymers Enables Transfection of Human Cells Comparable to Adenovirus. *Adv. Mater.* **2007**, *19*, 2836−2842.

(10) Theoharis, S.; Manunta, M.; Tan, P. H. Gene Delivery to Vascular Endothelium Using Chemical Vectors: Implications for Cardiovascular Gene Therapy. *Expert Opin. Biol. Ther.* **2007**, *7*, 627−643.

(11) Möckl, L.; Hirn, S.; Torrano, A. A.; Uhl, B.; Bräuchle, C.; Krombach, F. The Glycocalyx Regulates the Uptake of Nanoparticles by Human Endothelial Cells in Vitro. *Nanomedicine (London, U. K.)* **2017**, *12*, 207−217.

(12) Adamson, P. D.; Dweck, M. R.; Newby, D. E. The Vulnerable Atherosclerotic Plaque: In Vivo Identification and Potential Therapeutic Avenues. *Heart* **2015**, *101*, 1755−1766.

(13) Kheirolomoom, A.; Kim, C. W.; Seo, J. W.; Kumar, S.; Son, D. J.; Gagnon, M. K. J.; Ingham, E. S.; Ferrara, K. W.; Jo, H. Multifunctional Nanoparticles Facilitate Molecular Targeting and miRNA Delivery to Inhibit Atherosclerosis in ApoE(−/−) Mice. *ACS Nano* **2015**, *9*, 8885−8897.

(14) Chung, J.; Shim, H.; Kim, K.; Lee, D.; Kim, W. J.; Kang, D. H.; Kang, S. W.; Jo, H.; Kwon, K. Discovery of Novel Peptides Targeting Pro-Atherogenic Endothelium in Disturbed Flow Regions -Targeted siRNA Delivery to Pro-Atherogenic Endothelium in Vivo. *Sci. Rep.* **2016**, *6*, 25636.

(15) Nahrendorf, M.; Jaffer, F. A.; Kelly, K. A.; Sosnovik, D. E.; Aikawa, E.; Libby, P.; Weissleder, R. Noninvasive Vascular Cell Adhesion Molecule-1 Imaging Identifies Inflammatory Activation of Cells in Atherosclerosis. *Circulation* **2006**, *114*, 1504−1511.

(16) Tabas, I.; García-Cardeña, G.; Owens, G. K. Recent Insights Into the Cellular Biology of Atherosclerosis. *J. Cell Biol.* **2015**, *209*, 13−22.

(17) Collins, T.; Read, M. A.; Neish, A. S.; Whitley, M. Z.; Thanos, D.; Maniatis, T. Transcriptional Regulation of Endothelial Cell Adhesion Molecules: NF-Kappa B and Cytokine-Inducible Enhancers. *FASEB J.* **1995**, *9*, 899−909.

(18) Gareus, R.; Kotsaki, E.; Xanthoulea, S.; Van Der Made, I.; Gijbels, M. J. J.; Kardakaris, R.; Polykratis, A.; Kollias, G.; De Winther, M. P. J.; Pasparakis, M. Endothelial Cell-Specific NF-Kappa B Inhibition Protects Mice From Atherosclerosis. *Cell Metab.* **2008**, *8*, 372−383.

(19) Dagvadorj, J.; Naiki, Y.; Tumurkhuu, G.; Hassan, F.; Islam, S.; Koide, N.; Mori, I.; Yoshida, T.; Yokochi, T. Interleukin-10 Inhibits Tumor Necrosis Factor-Alpha Production in Lipopolysaccharide-Stimulated RAW 264.7 Cells Through Reduced Myd88 Expression. *Innate Immun.* **2008**, *14*, 109−115.

(20) Pinderski, L. J.; Fischbein, M. P.; Subbanagounder, G.; Fishbein, M. C.; Kubo, N.; Cheroutre, H.; Curtiss, L. K.; Berliner, J. A.; Boisvert, W. A. Overexpression of Interleukin-10 by Activated T Lymphocytes Inhibits Atherosclerosis in LDL Receptor-Deficient Mice by Altering Lymphocyte and Macrophage Phenotypes. *Circ. Res.* **2002**, *90*, 1064−1071.

(21) Liu, Y.; Li, D.; Chen, J.; Xie, J.; Bandyopadhyay, S.; Zhang, D.; Nemarkommula, A. R.; Liu, H.; Mehta, J. L.; Hermonat, P. L. Inhibition of Atherogenesis in LDLR Knockout Mice by Systemic Delivery of Adeno-Associated Virus Type 2-hIL-10. *Atherosclerosis* **2006**, *188*, 19−27.

(22) Kamaly, N.; Fredman, G.; Fojas, J. J. R.; Subramanian, M.; Choi, W. I.; Zepeda, K.; Vilos, C.; Yu, M.; Gadde, S.; Wu, J.; Milton, J.; Carvalho Leitao, R.; Rosa Fernandes, L.; Hasan, M.; Gao, H.; Nguyen, V.; Harris, J.; Tabas, I.; Farokhzad, O. C. Targeted Interleukin-10 Nanotherapeutics Developed With a Microfluidic Chip Enhance Resolution of Inflammation in Advanced Atherosclerosis. *ACS Nano* **2016**, *10*, 5280−5292.

DOI: 10.1021/acsabm.8b00342
ACS Appl. Bio Mater. XXXX, XXX, XXX−XXX

(23) Namiki, M.; Kawashima, S.; Yamashita, T.; Ozaki, M.; Sakoda, T.; Inoue, N.; Hirata, K.-I.; Morishita, R.; Kaneda, Y.; Yokoyama, M. Intramuscular Gene Transfer of Interleukin-10 cDNA Reduces Atherosclerosis in Apolipoprotein E-Knockout Mice. *Atherosclerosis* **2004**, *172*, 21−29.
(24) Wang, P.; Wu, P.; Siegel, M. I.; Egan, R. W.; Billah, M. M. Interleukin (IL)-10 Inhibits Nuclear Factor Kappa B (NF Kappa B) Activation in Human Monocytes. IL-10 and IL-4 Suppress Cytokine Synthesis by Different Mechanisms. *J. Biol. Chem.* **1995**, *270*, 9558−9563.
(25) Han, X.; Kitamoto, S.; Lian, Q.; Boisvert, W. A. Interleukin-10 Facilitates Both Cholesterol Uptake and Efflux in Macrophages. *J. Biol. Chem.* **2009**, *284*, 32950−32958.
(26) Niemand, C.; Nimmesgern, A.; Haan, S.; Fischer, P.; Schaper, F.; Rossaint, R.; Heinrich, P. C.; Müller-Newen, G. Activation of STAT3 by IL-6 and IL-10 in Primary Human Macrophages is Differentially Modulated by Suppressor Of Cytokine Signaling 3. *J. Immunol.* **2003**, *170*, 3263−3272.
(27) Riley, J. K.; Takeda, K.; Akira, S.; Schreiber, R. D. Interleukin-10 Receptor Signaling Through the JAK-STAT Pathway. Requirement for Two Distinct Receptor-Derived Signals for Anti-Inflammatory Action. *J. Biol. Chem.* **1999**, *274*, 16513−16521.
(28) Qin, H.; Holdbrooks, A. T.; Liu, Y.; Reynolds, S. L.; Yanagisawa, L. L.; Benveniste, E. N. SOCS3 Deficiency Promotes M1Macrophage Polarization and Inflammation. *J. Immunol.* **2012**, *189*, 3439−3448.
(29) Pike, K. A.; Hutchins, A. P.; Vinette, V.; Théberge, J.-F.; Sabbagh, L.; Tremblay, M. L.; Miranda-Saavedra, D. Protein Tyrosine Phosphatase 1B is a Regulator of the Interleukin-10-Induced Transcriptional Program in Macrophages. *Sci. Signaling* **2014**, *7*, Ra43.
(30) Sunshine, J. C.; Peng, D. Y.; Green, J. J. Uptake and Transfection With Polymeric Nanoparticles are Dependent on Polymer End-Group Structure, but Largely Independent of Nanoparticle Physical and Chemical Properties. *Mol. Pharmaceutics* **2012**, *9*, 3375−3383.
(31) Zhou, D.; Cutlar, L.; Gao, Y.; Wang, W.; O'Keeffe-Ahern, J.; Mcmahon, S.; Duarte, B.; Larcher, F.; Rodriguez, B. J.; Greiser, U.; Wang, W. The Transition From Linear to Highly Branched Poly(B-Amino Esters): Branching Matters for Gene Delivery. *Sci. Adv.* **2016**, *2*, 1600102.
(32) Robins, R. S.; Lemarié, C. A.; Laurance, S.; Aghourian, M. N.; Wu, J.; Blostein, M. D. Vascular Gas6 Contributes to Thrombogenesis and Promotes Tissue Factor Up-Regulation After Vessel Injury in Mice. *Blood* **2013**, *121*, 692−699.
(33) Kim, J.; Kang, Y.; Tzeng, S. Y.; Green, J. J. Synthesis and Application of Poly(Ethylene Glycol)-Co-Poly(B-Amino Ester) Copolymers for Small Cell Lung Cancer Gene Therapy. *Acta Biomater.* **2016**, *41*, 293−301.
(34) Williams, L.; Bradley, L.; Smith, A.; Foxwell, B. Signal Transducer And Activator Of Transcription 3 is the Dominant Mediator of the Anti-Inflammatory Effects of IL-10 in Human Macrophages. *J. Immunol.* **2004**, *172*, 567−576.
(35) Qin, H.; Wilson, C. A.; Roberts, K. L.; Baker, B. J.; Zhao, X.; Benveniste, E. N. IL-10 Inhibits Lipopolysaccharide-Induced CD40 Gene Expression Through Induction of Suppressor Of Cytokine Signaling-3. *J. Immunol.* **2006**, *177*, 7761−7771.
(36) Zhou, L.; Qu, X.; Guo, Y.; Wang, M.; Lei, B.; Ma, P. X. Branched Glycerol-Based Copolymer With Ultrahigh P65 siRNA Delivery Efficiency for Enhanced Cancer Therapy. *ACS Appl. Mater. Interfaces* **2018**, *10*, 4471−4480.
(37) Zhou, D.; Gao, Y.; Aied, A.; Cutlar, L.; Igoucheva, O.; Newland, B.; Alexeeve, V.; Greiser, U.; Uitto, J.; Wang, W. Highly Branched Poly(B-Amino Esters) for Skin Gene Therapy. *J. Controlled Release* **2016**, *244*, 336−346.
(38) Cutlar, L.; Zhou, D.; Gao, Y.; Zhao, T.; Greiser, U.; Wang, W.; Wang, W. Highly Branched Poly(B-Amino Esters): Synthesis and Application in Gene Delivery. *Biomacromolecules* **2015**, *16*, 2609−2617.
(39) Liu, S.; Gao, Y.; A, S.; Zhou, D.; Greiser, U.; Guo, T.; Guo, R.; Wang, W. Biodegradable Highly Branched Poly(B-Amino Esters) for Targeted Cancer Cell Gene Transfection. *ACS Biomater. Sci. Eng.* **2017**, *3*, 1283−1286.
(40) Huang, J.-Y.; Gao, Y.; Cutlar, L.; O'Keeffe-Ahern, J.; Zhao, T.; Lin, F.-H.; Zhou, D.; Mcmahon, S.; Greiser, U.; Wang, W.; Wang, W. Tailoring Highly Branched Poly(B-Amino Esters): A Synthetic Platform for Epidermal Gene Therapy. *Chem. Commun. (Cambridge, U. K.)* **2015**, *51*, 8473−8476.
(41) Gao, Y.; Huang, J.-Y.; O'Keeffe Ahern, J.; Cutlar, L.; Zhou, D.; Lin, F.-H.; Wang, W. Highly Branched Poly(B-Amino Esters) for Non-Viral Gene Delivery: High Transfection Efficiency and Low Toxicity Achieved by Increasing Molecular Weight. *Biomacromolecules* **2016**, *17*, 3640−3647.
(42) Smith, T. T.; Stephan, S. B.; Moffett, H. F.; Mcknight, L. E.; Ji, W.; Reiman, D.; Bonagofski, E.; Wohlfahrt, M. E.; Pillai, S. P. S.; Stephan, M. T. In Situ Programming of Leukaemia-Specific T Cells Using Synthetic DNA Nanocarriers. *Nat. Nanotechnol.* **2017**, *12*, 813−820.
(43) Park, H.-J.; Lee, J.; Kim, M.-J.; Kang, T. J.; Jeong, Y.; Um, S. H.; Cho, S.-W. Sonic Hedgehog Intradermal Gene Therapy Using a Biodegradable Poly(B-Amino Esters) Nanoparticle to Enhance Wound Healing. *Biomaterials* **2012**, *33*, 9148−9156.
(44) Gu, J.; Wang, X.; Jiang, X.; Chen, Y.; Chen, L.; Fang, X.; Sha, X. Self-Assembled Carboxymethyl Poly (L-Histidine) Coated Poly (B-Amino Ester)/DNA Complexes for Gene Transfection. *Biomaterials* **2012**, *33*, 644−658.
(45) Chung, E. J.; Tirrell, M. Recent Advances in Targeted, Self-Assembling Nanoparticles to Address Vascular Damage Due to Atherosclerosis. *Adv. Healthcare Mater.* **2015**, *4*, 2408−2422.
(46) Kelley, W. J.; Safari, H.; Lopez-Cazares, G.; Eniola-Adefeso, O. Vascular-Targeted Nanocarriers: Design Considerations and Strategies for Successful Treatment of Atherosclerosis and Other Vascular Diseases. *Wiley Interdiscip Rev. Nanomed Nanobiotechnol* **2016**, *8*, 909−926.
(47) Ma, S.; Tian, X. Y.; Zhang, Y.; Mu, C.; Shen, H.; Bismuth, J.; Pownall, H. J.; Huang, Y.; Wong, W. T. E-Selectin-Targeting Delivery of MicroRNAs by Microparticles Ameliorates Endothelial Inflammation and Atherosclerosis. *Sci. Rep.* **2016**, *6*, 22910.
(48) Mastorakos, P.; Da Silva, A. L.; Chisholm, J.; Song, E.; Choi, W. K.; Boyle, M. P.; Morales, M. M.; Hanes, J.; Suk, J. S. Highly Compacted Biodegradable DNA Nanoparticles Capable of Overcoming the Mucus Barrier for Inhaled Lung Gene Therapy. *Proc. Natl. Acad. Sci. U. S. A.* **2015**, *112*, 8720−8725.
(49) Zhou, J.; Liu, J.; Cheng, C. J.; Patel, T. R.; Weller, C. E.; Piepmeier, J. M.; Jiang, Z.; Saltzman, W. M. Biodegradable Poly(Amine-Co-Ester) Terpolymers for Targeted Gene Delivery. *Nat. Mater.* **2012**, *11*, 82−90.
(50) Harris, T. J.; Green, J. J.; Fung, P. W.; Langer, R.; Anderson, D. G.; Bhatia, S. N. Tissue-Specific Gene Delivery Via Nanoparticle Coating. *Biomaterials* **2010**, *31*, 998−1006.
(51) Tzeng, S. Y.; Yang, P. H.; Grayson, W. L.; Green, J. J. Synthetic Poly(Ester Amine) and Poly(Amido Amine) Nanoparticles for Efficient DNA and Sirna Delivery to Human Endothelial Cells. *Int. J. Nanomed.* **2011**, *6*, 3309−3322.
(52) Hovsepian, E.; Penas, F.; Siffo, S.; Mirkin, G. A.; Goren, N. B. IL-10 Inhibits the NF-KB and ERK/MAPK-Mediated Production of Pro-Inflammatory Mediators by Up-Regulation of SOCS-3 in Trypanosoma Cruzi-Infected Cardiomyocytes. *PLoS One* **2013**, *8*, 79445.
(53) Sun, L.; Louie, M. C.; Vannella, K. M.; Wilke, C. A.; Levine, A. M.; Moore, B. B.; Shanley, T. P. New Concepts of IL-10-Induced Lung Fibrosis: Fibrocyte Recruitment and M2 Activation in a CCL2/CCR2 Axis. *Am. J. Physiol. Lung Cell Mol. Physiol.* **2011**, *300*, L341−53.
(54) Han, X.; Boisvert, W. A. Interleukin-10 Protects Against Atherosclerosis by Modulating Multiple Atherogenic Macrophage Function. *Thromb. Haemostasis* **2015**, *113*, 505−512.

DOI: 10.1021/acsabm.8b00342
ACS Appl. Bio Mater. XXXX, XXX, XXX−XXX

(55) Mizuguchi, H.; Xu, Z.; Ishii-Watabe, A.; Uchida, E.; Hayakawa, T. IRES-Dependent Second Gene Expression is Significantly Lower Than Cap-Dependent First Gene Expression in a Bicistronic Vector. *Mol. Ther.* **2000**, *1*, 376−382.
(56) Qasimi, P.; Ming-Lum, A.; Ghanipour, A.; Ong, C. J.; Cox, M. E.; Ihle, J.; Cacalano, N.; Yoshimura, A.; Mui, A. L.-F. Divergent Mechanisms Utilized by SOCS3 to Mediate Interleukin-10 Inhibition of Tumor Necrosis Factor Alpha and Nitric Oxide Production by Macrophages. *J. Biol. Chem.* **2006**, *281*, 6316−6324.
(57) Clarke, C. J.; Hales, A.; Hunt, A.; Foxwell, B. M. IL-10-Mediated Suppression of TNF-Alpha Production is Independent of Its Ability to Inhibit NF Kappa B Activity. *Eur. J. Immunol.* **1998**, *28*, 1719−1726.
(58) Nam, J.; Aguda, B. D.; Rath, B.; Agarwal, S. Biomechanical Thresholds Regulate Inflammation Through the NF-Kappa B Pathway: Experiments and Modeling. *PLoS One* **2009**, *4*, e5262.
(59) He, H.; Lancina, M. G.; Wang, J.; Korzun, W. J.; Yang, H.; Ghosh, S. Bolstering Cholesteryl Ester Hydrolysis in Liver: A Hepatocyte-Targeting Gene Delivery Strategy for Potential Alleviation of Atherosclerosis. *Biomaterials* **2017**, *130*, 1−13.

DOI: 10.1021/acsabm.8b00342
ACS Appl. Bio Mater. XXXX, XXX, XXX−XXX